An H I interstellar bubble surrounding WR 85 and RCW 118

J. Vasquez,[1][*][†] C. Cappa[1,2][‡] and N. M. McClure-Griffiths[3]

[1]*Instituto Argentino de Radioastronomía, C.C.5. 1894, Villa Elisa, Argentina*
[2]*Facultad de Ciencias Astronómicas y Geofísicas, Universidad Nacional de La Plata, La Plata, Argentina*
[3]*Australia Telescope National Facility, CSIRO, PO Box 76, Epping NSW 1710, Australia*

ABSTRACT

We analyse the distribution of the interstellar matter in the environs of the Wolf-Rayet star LSS 3982 (= WR 85, WN6+OB?) linked to the optical ring nebula RCW 118. Our study is based on neutral hydrogen 21-cm line data belonging to the Southern Galactic Plane Survey (SGPS).

The analysis of the H I data allowed the identification of a neutral hydrogen interstellar bubble related to WR 85 and the 25-arcmin-diameter ring nebula RCW 118. The H I bubble was detected at a systemic velocity of -21.5 km s^{-1}, corresponding to a kinematical distance of 2.8 ± 1.1 kpc, compatible with the stellar distance. The neutral structure is about 25 arcmin in radius or 21 ± 8 pc, and is expanding at 9 ± 2 km s^{-1}. The associated ionized and neutral masses amount to 3000 M$_\odot$. The carbon monoxide (CO) emission distribution depicts a region lacking CO coincident in position and velocity with the H I structure. The 9.3-arcmin-diameter inner optical nebula appears to be related to the approaching part of the neutral atomic shell. The H I void and shell are the neutral gas counterparts of the optical bubble and have very probably originated in the action of the strong stellar wind of the central star during the O-type and WR phases on the surrounding interstellar medium. The H I bubble appears to be in the momentum conserving stage.

Key words: stars: Wolf–Rayet – ISM: bubbles – ISM: H II regions.

1 INTRODUCTION

Wolf-Rayet (WR) stars are the evolutionary descendents of massive O-type stars. With mass loss rates in the interval $(1-5) \times 10^{-5}$ M$_\odot$ yr^{-1} and terminal velocities of 1000–3000 km s^{-1} (van der Hucht 2001; Cappa, Goss & van der Hucht 2004), these hot and luminous stars are one of the most powerful stellar wind sources in our Galaxy. Of-type stars are also characterized by high mass loss rates and terminal velocities (Prinja, Barlow & Howarth 1990; Lamers & Leitherer 1993).

The mechanical energy released to the interstellar medium (ISM) during the WR phase only ($t_{WR} \lesssim 7 \times 10^5$ yr; Meynet & Maeder 2003) is in the range $(1-30) \times 10^{50}$ erg, comparable to the mechanical energy injected during a supernova explosion. Both the mass flow from the WR star and the previous O-type star phases strongly modify the energetics, the morphology and the chemical abundances of the ISM in the environs of the star.

The interaction of the strong stellar winds with the surrounding interstellar matter has been analysed by several authors, taking into account different environments (e.g. García-Segura & Mac Low 1995). The stellar flow sweeps up the surrounding material creating *interstellar bubbles*, which are detected at different wavelengths from the UV to the radio range. In the optical regime, these structures are generally observed as filamentary ring nebulae in the light of Hα and [O III] (e.g. Chu, Treffers & Kwitter 1983; Marston et al. 1994b). They are related to many WR stars and to a relatively large number of O and Of stars. Shell-shaped structures created by stellar winds from massive stars are also identified in the far infrared and in the thermal radio continuum emission (e.g. Mathis et al. 1992; Cappa, Goss & Pineault 2002).

Interstellar bubbles appear as cavities and expanding shells in the neutral hydrogen 21-cm line emission distribution (e.g. Cappa et al. 2003, and references therein). H I bubbles are external to their optical and radio continuum counterparts, and expand at relatively low velocities ($\lesssim 10$ km s^{-1}). In most of the cases, the derived dynamical ages are larger than the duration of the WR phase, suggesting that the stellar winds of the massive O-type star progenitor has also contributed to creating the structures.

As part of a systematic search for neutral gas bubbles around massive stars, we present here a study of the ISM surrounding WR 85 (=HD 155603B = LSS 3982) based mainly on H I 21-cm line data belonging to the Southern Galactic Plane Survey (SGPS) and additional molecular and radio continuum data.

---

[*]Fellow of CONICET, Argentina.
[†]E-mail: pete@tux.iar.unlp.edu.ar
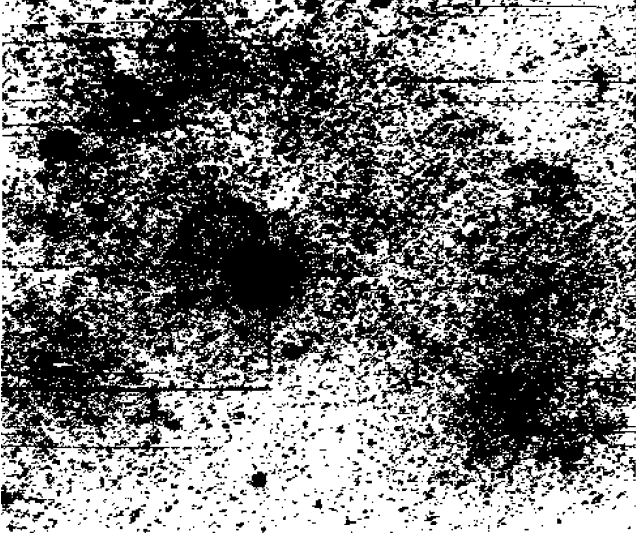[‡]Member of Carrera del Investigador, CONICET, Argentina.

Figure 1. Hα image in (α, δ) coordinates showing the two concentric rings around WR 85 (taken from Marston et al. 1994b). North is up and East is to the left.

WR 85 is classified as WN6h + OB?. Different distance estimates have been published for this star. WR 85 belongs to the HD 155603 group, for which Moffat & FitzGerald (1977) found a distance of 1.8 kpc. Conti & Vacca (1990) and van der Hucht (2001) locate the star at $d = 3.7 \pm 1.3$ and 4.7 ± 2.3 kpc, respectively, while *Hipparcos* measurements indicate 1.7 kpc. The X-ray point like source 1 WGA J1714.4-3949 coincides in position with the WR star (Pfeffermann & Aschenbach 1996).

HD 155603B is associated with the optical ring nebula RCW 118, of about 25 arcmin in diameter (Chu & Treffers 1981; Heckathorn, Bruhweiler & Gull 1982; Marston et al. 1994a,b). Chu et al. (1983) observed RCW 118 with the Curtis-Schmidt-0.6-m telescope at Cerro Tololo Inter-American Observatory (CTIO) in Hα, [O III]λ5007 and [S II]λ6730. These authors found that the ionized gas in the nebula has an LSR velocity of $-15\,\mathrm{km\,s^{-1}}$, and derived an expansion velocity $\leqq 10\,\mathrm{km\,s^{-1}}$ and a dynamical age of 6.7×10^5 yr, compatible with the duration of the WR phase. Based on the velocity of the ionized gas and on standard galactic rotation models, they estimated a kinematical distance $d_k \sim 2.3$ kpc.

Marston et al. (1994b) reobserved the nebula using the same telescope. Their Hα image reveals the presence of two semicircular rings. The inner ring has a diameter of 9.3 arcmin, and is centred on the WR star, whereas the outer one, 25 arcmin in diameter, is centred slightly to the south and south-east of the star. The two concentric structures can be clearly identified in the Hα image displayed in Fig. 1.

RCW 118 is in the same line of sight to the SNR G347.3–0.5, discovered in the *ROSAT* All Sky Survey (RASS) by Pfeffermann & Aschenbach (1996). This SNR, 1° in diameter, is located at ≈ 6 kpc (see Lazendic et al. 2004).

2 DATA BASES

The H I 21-cm line emission data used in this paper belong to the SGPS (McClure-Griffiths et al. 2005) obtained with the Australia Telescope Compact Array (ATCA) and the Parkes radiotelescope (short spacing information). The H I data cube is centred at $(l, b, v) = (347°14', -0°29', -40\,\mathrm{km\,s^{-1}})$, covers a region of about

Table 1. H I data: main observational parameters.

(l, b) centre	$347°14', -0°29'$
Velocity range	$-204, 124\,\mathrm{km\,s^{-1}}$
Velocity resolution	$1.64\,\mathrm{km\,s^{-1}}$
Surveyed area	$2° \times 2°$
RMS noise	1.3 K
Synthesized beam (arcmin)	2.6×2.1

$2° \times 2°$ around the WR star and has a synthesized beam of 2.6×2.1 arcmin. To improve the signal-to-noise ratio, we applied a Hanning smoothing to the individual line images. Consequently, the original rms noise level of 2.4 K was lowered to 1.3 K and the channel velocity resolution was doubled. The main observational parameters of the final data cube are summarized in Table 1.

Additional infrared, radio continuum and molecular data were also analysed. High-resolution infrared images (HIRES) were obtained from IPAC.[1] The *IRAS* data, obtained at 12, 25, 60 and 100 μm, have angular resolutions in the range 0.5 to about 2 arcmin. Radio continuum data at 2.4 GHz were obtained from the survey by Duncan et al. (1995) with an angular resolution of 10.4 arcmin. The molecular data correspond to the carbon monoxide (CO; $J = 1 \rightarrow 0$) line at 115 GHz and belong to the CO survey by Dame, Hartmann & Thaddeus (2001), with angular and velocity resolutions of 9 arcmin and $1.3\,\mathrm{km\,s^{-1}}$, respectively, and an rms noise of 0.3 K.

3 IONIZED AND NEUTRAL GAS DISTRIBUTION TOWARDS WR 85

3.1 H I line emission distribution

The strong stellar winds from massive stars are expected to sweep-up the interstellar material around the wind source and to create a highly evacuated region surrounded by an expanding shell. If the ionizing front is trapped within the envelope, the void and the surrounding shell are expected to appear as a region lacking neutral material encircled by regions of enhanced H I emission. The analysis of the neutral gas emission distribution in the environs of these stars allows identification of such cavities and surrounding shells associated with the wind sources.

The criteria adopted to relate an H I cavity and shell to a certain star are (i) the star should be located close to the centre of the void or within the inner border of the H I surrounding shell; (ii) the ionized ring nebula, if present, should appear projected within the cavity or close to the inner border of the neutral shell and (iii) the kinematical distance to the H I structure should be compatible, within errors, with the stellar distance.

To facilitate the visualization of the general characteristics of the H I emission in the line of sight to this region of the Galaxy, we show the average H I profile corresponding to an area of $1° \times 1°$ centred at the position of WR 85 in the top panel of Fig. 2. The bottom panel shows a plot of the kinematical distance d_k *versus* the LSR radial velocity for the galactic longitude $l = 347°$, as obtained from the circular galactic rotation model by Brand & Blitz (1993).

Brightness temperatures higher than a few Kelvins are observed for velocities spanning the range -130 to $+50\,\mathrm{km\,s^{-1}}$. According to
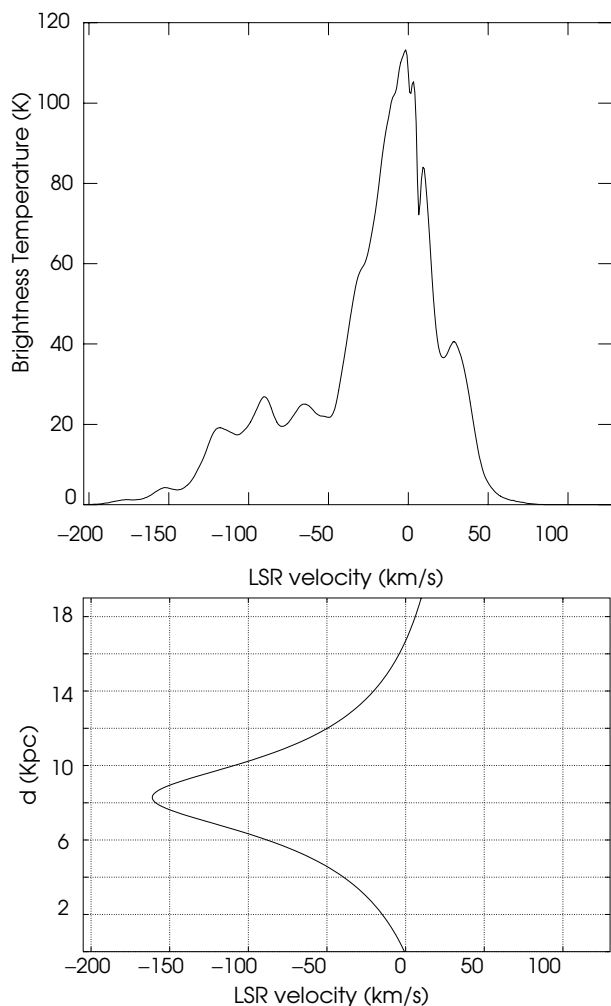

Figure 2. *Top panel:* Average H I brightness temperature spectrum *versus* LSR velocity, corresponding to an area of $1° \times 1°$ centred at the position of WR 85. *Bottom panel:* Kinematical distance *versus* LSR velocity plot obtained from the analytical fit to the circular galactic rotation model by Brand & Blitz (1993) for $l = 347°$.

the quoted circular galactic rotation model, gas at negative velocities is placed at kinematical distances $d_k \approx 0$–7 kpc or $d_k \geqq 9$ kpc, while positive velocities are forbidden for distances closer than 17 kpc. Gas within the near distance range is most probably related to the Local and the Carina-Sagittarius arms (Georgelin & Georgelin 1976).

To analyse in some detail the neutral atomic gas distribution in the environs of the WR star, we obtained a series of H I line images at constant velocities, paying particular attention to the gas distribution at negative velocities. The analysis of the neutral atomic gas distribution within the velocity range -150–0 km s^{-1} shows a clear void with the star projected close to its centre at velocities of about -21 km s^{-1}.

The top panel of Fig. 3 displays the H I column density distribution within the velocity interval -28.0 to -16.5 km s^{-1}, where the void is clearly detected. The void appears surrounded by an almost circular shell. The centroid of the structure, defined following the maxima in the shell is placed at $(l, b) = (347°26', -0°37')$, close to the position of WR 85 (indicated by the star symbol). The brightness temperature gradient of the structure is slightly steeper towards the galactic plane than towards the other sections of the shell, indicating the presence of higher density regions close to $b = 0°$.
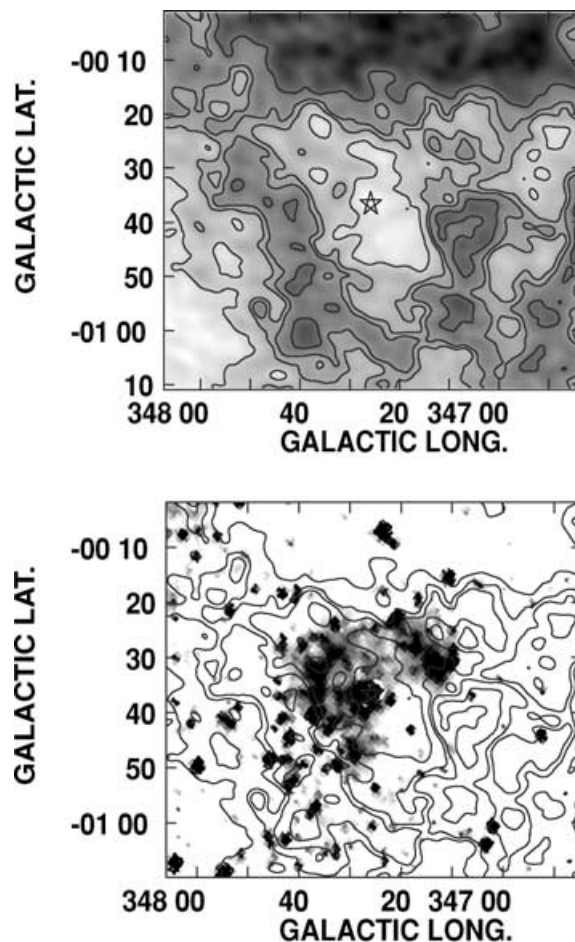
Figure 3. *Top panel:* H I column density distribution surrounding WR 85 within the velocity interval -28.0 to -16.5 km s^{-1}. The grey-scale corresponds to $(1.2$–$1.7) \times 10^{21}$ cm^{-2} and the contour lines are 1.2, 1.4, 1.5 and 1.6×10^{21} cm^{-2}. The star symbol indicates the position of the WR star. *Bottom panel:* Overlay of the SHASSA Hα image of the nebula and the same H I contours of the top panel. Hα units are arbitrary.

The bottom panel of Fig. 3 displays a superposition of the Hα image of the region obtained from the Southern H-alpha Sky Survey Atlas (SHASSA) (Gaustad et al. 2001) (*grey-scale*) and the same H I contours of the top panel. The 25-arcmin-diameter outer nebula is clearly detected in the optical image (see Fig. 1 for a comparison), while the 9.3-arcmin-diameter inner nebula is barely identified. The bottom panel of Fig. 3 shows that the 25-arcmin-diameter optical nebula is projected onto the H I cavity and close to the inner border of the H I shell.

The systemic velocity of the structure, defined as the velocity at which the H I cavity presents its largest dimensions and deepest temperature gradient, is $v_{sys} \approx -21$ km s^{-1}. This value is compatible, within errors, with the velocity of the ionized gas found by Chu & Treffers (1981) (-15 km s^{-1}).

The presence of the outer optical nebula close to the inner border of the H I shell and the morphological agreement between RCW 118 and the H I emission, along with the agreement between the systemic velocity of the H I structure and the velocity of the ionized gas, indicate that the H I feature is related to RCW 118.

Fig. 4 displays two profiles showing the H I column density *versus* the galactic longitude for $b = -0°36'$ (*thin line*) and the galactic latitude for $l = 347°25'$ (*thick line*). This plot clearly shows that the
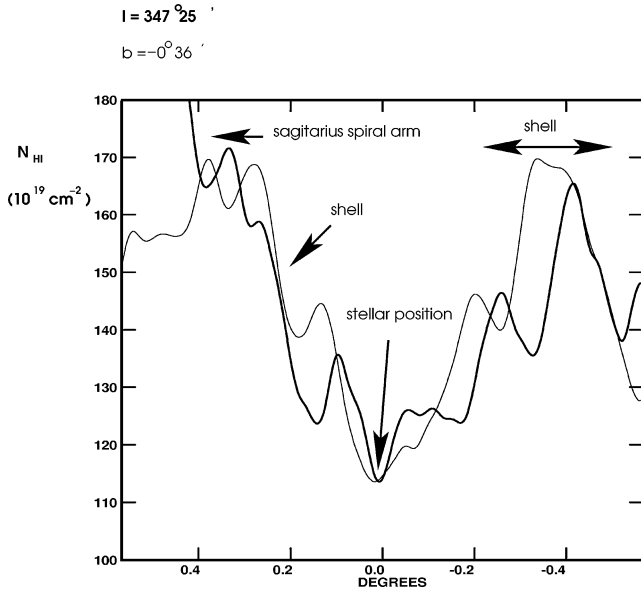
Figure 4. Profiles showing the H I column density within the velocity interval -28.0 to -16.5 km s^{-1} *versus* galactic longitude obtained at $b = -0°36'$ (thin line) and *versus* galactic latitude at $l = 347°25'$ (thick line). The x-axis is referred to the stellar position.

WR star is projected onto a minimum in the H I emission distribution. The neutral shell is identified with arrows. The wide line shows that although most of the neutral gas near $b = 0°$ is linked to the Sagittarius arm, it is unconnected to the H I feature shown in Fig 3.

We analysed in some detail the H I gas distribution in the close environs of the 9.3-arcmin optical ring. The top panel of Fig. 5 displays the neutral gas emission distribution for the velocity interval -29.3 to -27.6 km s^{-1} (in grey-scale and coutour lines), while the bottom panel shows an overlay of the optical image (grey-scale) and the H I emission distribution (contour lines). The figure reveals the presence of neutral gas emission closely bordering the inner semicircular optical ring. The morphological correlation between the H I emission and the border of the inner nebula suggests that the ionized and the neutral material are related. Some correlation between the inner optical ring and neutral hydrogen is also detected at velocities spanning the range -27.6 to -25.2 km s^{-1}. This H I gas is also shown as the H I peaks interior to the H I shell detected about 10 arcmin far from the star in the profiles in Fig. 4.

The velocity interval at which the correlation between the inner ring and the H I cloud is better detected suggests that the inner optical nebula is located on the approaching section of the expanding shell associated with RCW 118.

3.2 Radio continuum emission

Fig. 6 displays an overlay between the radio continuum emission at 2.4 GHz (contour lines) and the H I column density distribution (grey-scale). Within the region of interest, the figure shows a radio source centred at $(l, b) = (347°32', -0°29')$, coincident with the brightest section of RCW 118 and with the inner optical ring located close to the star. Weak radio emission can also be detected towards higher negative galactic latitudes and lower galactic longitudes, coincident with fainter regions of RCW 118. The positional coincidence between both the radio source and the weak radio emission, and RCW 118 suggests that the emission at 2.4 GHz originates in the ionized nebular gas.
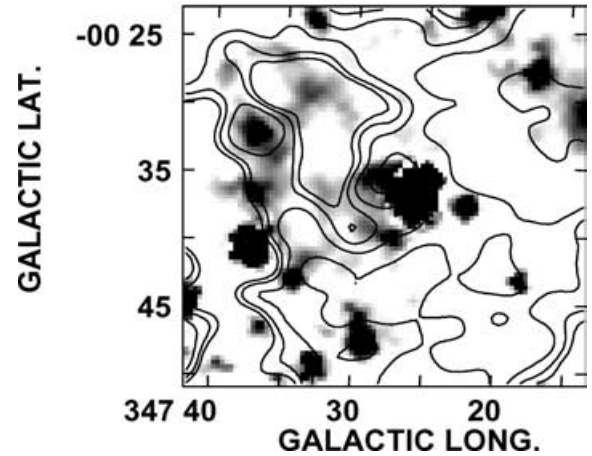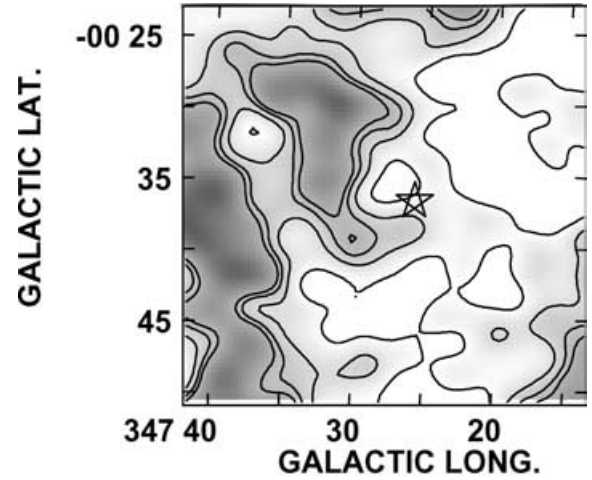

Figure 5. *Top panel:* H I emission distribution within the velocity interval -29.3 to -27.6 km s^{-1} in grey-scale and contour lines. The grey-scale corresponds to 45–90 K. The contour lines are 45, 50, 53, 55 K. The cross marks the position of the WR star. *Bottom panel:* Overlay of the SHASSA Hα image and the same H I contours of the top panel.

An image at 4.85 GHz can be obtained from the PMN Survey (Condon et al. 1995). However, the presence of extended areas lacking radio data within the region of interest does not make this image useful. The presence of weak radio emission in this region is also evident at 4.85 GHz in the survey by Haynes, Caswell & Simons (1978).

3.3 Molecular and IR emission

The left panel of Fig. 7 shows the CO($J = 1 \rightarrow 0$) line emission distribution within the velocity range -32.5 to -24.7 km s^{-1} taken from the Dame et al. (2001) survey. The stellar position is indicated by the star. A region of low molecular emission, $\sim 1°30' \times 0°45'$ in size, centred near $(347°25', -0°36')$ is evident in the image. The right panel of the figure displays an enlargement of the molecular void showing an overlay of the CO emission distribution (thick contour lines) and the H I column density image of Fig. 3 (grey-scale and thin contour lines).
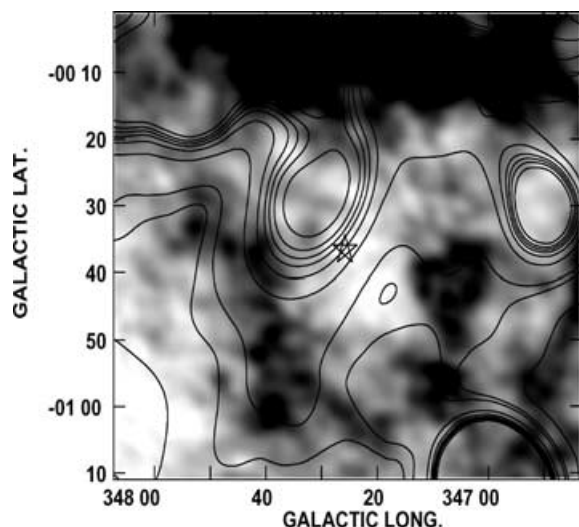
Figure 6. Overlay of the radio continuum image at 2.4 GHz (contour lines) and the H I column density distribution (grey-scale). The star marks the position of WR 85. Contour lines are 0.5, 1.0, 1.2, 2.0, 2.5, 2.8, 3.0 and 0.32 Jy beam.

The image on the right shows the clear correspondence between the H I structure and the higher galactic longitude section of the CO cavity at $l > 347°00'$. Note that the CO maxima are external to the H I shell, suggesting that some stratification in the gas density is present. The section of the molecular cavity at $l < 347°00'$, which is wider in galactic latitude, is not linked to the interstellar bubble.

The HIRES *IRAS* images at 12, 25, 60 and 100 μm do not show any structure connected either to the optical or to the H I and CO shells. Only an IR emission gradient probably linked to the galactic plane is present in the images at 60 and 100 μm.

4 THE H I BUBBLE RELATED TO WR 85 AND RCW 118

4.1 The distance

The kinematical distance d_k to the H I structure was estimated from the analytical fit to the circular galactic rotation model by Brand & Blitz (1993).

This model predicts that gas at $v_{sys} = -21$ km s^{-1} should be located at 2.7 ± 0.7 or 14 ± 1 kpc. The uncertainties in the quoted values were estimated by assuming the presence of non-circular motions of ≈ 6 km s^{-1}. The near kinematical distance estimate is compatible with the kinematical distance of the ionized gas ($d_k = 2.0$ kpc) derived using the same model.

Bearing in mind the available photometric data for WR 85 and the intrinsic colour and absolute magnitude corresponding to a WN 6 star from van der Hucht (2001), the spectrophotometric distance estimate is $d \approx 2.2 \pm 0.9$ kpc, where the uncertainty in the stellar distance corresponds to the error in the absolute magnitude (± 0.9 mag). This distance estimate is consistent with the near kinematical distance derived from H I data.

van der Hucht (2001) suggests the existence of an OB companion to WR 85. However, the absence of OB absorption lines in the spectrum of WR 85 (Gamen, private communication) suggests that the OB companion would be at least 2.5 mag weaker than the WR star. Consequently, a correction factor to the apparent magnitude of WR 85 has not been taken into account.

Bearing in mind these values and the distances derived by different authors (see Section 1), we adopted $d_k = 2.8 \pm 1.1$ kpc for both the optical and the H I structures. The uncertainty in the adopted distance is 40 per cent.

The agreement in position, velocity and distance among the WR star, RCW 118 and the H I feature suggests that the H I structure is associated with the outer optical ring nebula. The presence of a central star characterized by a strong mass flow inside the H I structure and the optical nebula suggests that the stellar wind of the WR star and its massive progenitor may have had an important role in shaping the nebula. We therefore interpret the H I structure as the neutral gas counterpart of the optical interstellar bubble.

4.2 Main parameters of the interstellar bubble around WR 85

The physical parameters of the H I bubble are summarized in Table 2. The centroid of the structure was defined taking into account the position of the maxima in the shell.

The velocity range corresponds to the velocity interval where the structure is detected. The systemic velocity was defined in Section 3.1. The expansion velocity was estimated as $v_{exp} = (v_2 - v_1)/2 + 1.6$ km s^{-1} and represents a lower limit to
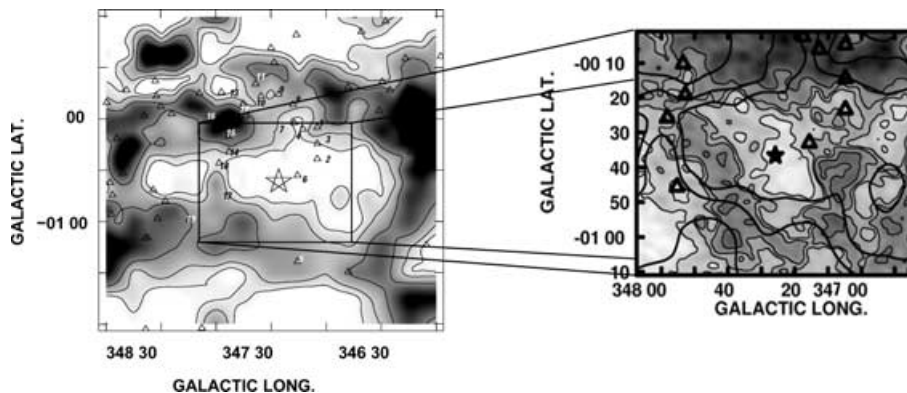

Figure 7. *Left panel:* Mean brightness temperature corresponding to the CO emission distribution within the velocity interval -32.5 to -24.7 km s^{-1}. The grey-scale corresponds to 0.2 to 1.7 K. The contour lines are 0.3, 0.5 and 0.9 K. The cross marks the position of the WR star. The triangles mark the location of *IRAS* protostellar candidates (see text). *Right panel:* Enlargement of the central region of the image on the left showing an overlay of the H I (*grey-scale and thin contour lines)* and the CO (*thick contour lines)* emissions. The star symbol indicates the stellar position. The triangles mark the location of *IRAS* protostellar candidates.

Table 2. Physical parameters of the H I bubble.

(l, b) centroid	$347°26', -0°37'$
Velocity range $v_2, v_1 (\text{km s}^{-1})$	$-28.0, -16.5$
Systemic velocity (km s^{-1})	-21 ± 5
Expansion velocity (km s^{-1})	9 ± 2
Angular radius of the H I cavity	20 arcmin
Angular radius of the H I shell	30 arcmin
Angular radius of the H I bubble	25 arcmin
Adopted distance (kpc)	2.8 ± 1.1
Linear radius of the H I bubble (pc)	21 ± 8
H I mass deficiency of the cavity ($M_\odot$)	220 ± 170
H I mass in the shell ($M_\odot$)	830 ± 780
H I mass in the H I bubble ($M_\odot$)	530 ± 400
Swept-up neutral mass ($M_\odot$)	720 ± 570
Dynamical age (yr)	$(\sim 1.1 \pm 0.5) \times 10^6$

the true expansion velocity. The extra 1.6 km s^{-1} allows for the presence of H I in the undetected caps of the expanding shell. Because of its small column density, these caps are difficult to identify in the fore- and background emission.

The cavity was defined following the contour line corresponding to $1.4 \times 10^{21} \text{ cm}^{-2}$ (see Fig. 3). The angular radius of the shell corresponds approximately to the outer border of the envelope. It can be clearly established for $b < -0°25'$, while confusion with fore- and background gas precludes the identification of the shell near $b < -0°10'$. The size of the bubble was estimated through the maxima in the shell.

The H I mass deficiency in the cavity and the H I mass in the shell were obtained from the column density image shown in Fig. 3. The swept-up neutral mass associated with the H I bubble was derived as a mean value between the mass deficiency in the cavity and the mass in the shell assuming a 10 per cent He abundance.

Bearing in mind an error of 40 per cent in the adopted distance, uncertainties in radii and masses are about 40 per cent and 80 per cent, respectively.

Evolutionary models of interstellar bubbles allow an estimate of the dynamical age as $t_d = 0.50 \times 10^6 \ R/v_{exp}$ yr (McCray 1983), corresponding to the momentum conserving stage of an interstellar bubble, where R is the radius of the bubble (pc), v_{exp} is the expansion velocity (km s^{-1}) and the constant is the deceleration parameter. The derived dynamical age, $t_d = 1.1 \times 10^6$ yr, is larger than the duration of the WN phase of a massive star ($t_{WN} = 0.3 \times 10^6$ yr for a rotating star of 40 $M_\odot$, Meynet & Maeder 2003) and suggests that the O-type star progenitor of the present WR star has contributed in the formation of the bubble.

A rough estimate of the ionized mass M_i and the electron density n_e related to RCW 118 was obtained from the radio continuum image at 2.4 GHz (Fig. 6) using the classical expressions by Mezger & Henderson (1967) for the case of a spherical H II region. We derived the flux density by assuming that the strong radio source at $347°32', -0°29'$ and part of the weak radio emission towards higher negative galactic latitudes and lower galactic longitudes is related to RCW 118. For a flux density $S_{2.4} = 12$ Jy, and assuming an electron temperature of 10^4 K, and a filling factor $f = 0.35-0.45$, we derived $M_i = 2100-2400 \, M_\odot$ and $n_e = 13-15 \text{ cm}^{-3}$. The filling factor was estimated from the optical image and corresponds to an ionized shell of about 13 arcmin in radius and 4 arcmin in thickness. We assume that about 50–70 per cent of the shell surface is covered by gas. Uncertainties in the ionized masses

and electron densities are about 80 per cent. We have also assumed that He is singly ionized.

Taking into account the neutral atomic and the ionized masses, the total mass in the interstellar bubble is $M_s \sim 3000 \, M_\odot$. The average ambient density estimated by distributing the total mass within a volume of 21 pc in radius is $\sim 3 \text{ cm}^{-3}$.

It is not clear whether part of the molecular material that encircles both the H I and the H II shells participates in the expansion. An estimate of the amount of molecular gas can be obtained from Fig. 7 by applying the empirical relation between $W_{CO} (= \int T_{mb} dv)$ and the H_2 column density $N_{H_2} = (1.1 \pm 0.2) \times 10^{20} \times W_{CO} \text{ cm}^{-2} (\text{K km s}^{-1})^{-1}$, obtained from γ-ray studies of molecular clouds in the IV galactic quadrant (Slane et al. 1999). The total H_2 mass is estimated to be 6800 $M_\odot$.

4.3 The energetics

An estimate of the mechanical luminosity $L_w (= \dot{M} V_w^2 / 2)$ of the stellar wind of WR 85 can be obtained by assuming a typical mass loss rate $\dot{M} = 2 \times 10^{-5} \, M_\odot \text{ yr}^{-1}$ for the WN phase (Cappa et al. 2004) and a terminal velocity $V_w = 1430 \text{ km s}^{-1}$ (Rochowicz & Nieldzieski 1995). For the previous main sequence O-type star phase, we adopted $\dot{M} = 2 \times 10^{-6} \, M_\odot \text{ yr}^{-1}$ and a terminal velocity $V_w = 1000 \text{ km s}^{-1}$ (Prinja, Fullerton & Crowther 1996). Mechanical luminosities corresponding to the WR and the O-type star phases turn out to be $L_{WR} = 1.3 \times 10^{37} \text{ erg s}^{-1}$ and $L_O = 6.3 \times 10^{35} \text{ erg s}^{-1}$. Assuming a typical lifetime for the WN phase $t_{WN} = 0.3 \times 10^6$ yr (Meynet & Maeder 2003) and for the O-type phase $t_O = 3 \times 10^6$ yr (Conti & Vacca 1990), the total stellar wind mechanical energy transferred to the ISM is $E_w = 1.8 \times 10^{50}$ erg. A similar value (1.2×10^{50} erg) is derived assuming that the stellar wind of the WR star and the previous O-type star phase have blown the gas bubble during 0.3×10^6 and 0.8×10^6 yr, respectively. These lifetimes are compatible with the derived dynamical age. Taking into account the large uncertainty in the dynamical age, we believe that the derived E_w values can be considered as the lower and upper limits to the true stellar wind energy.

The kinetic energy $E_k (= M_s V_{exp}^2 / 2)$ in the interstellar bubble derived taking into account the expansion velocity from Table 2 and the swept-up atomic neutral and ionized masses is $E_k = 8.3 \times 10^{48}$ erg. If the molecular material also participates in the expansion, $E_k = 8.8 \times 10^{48}$ erg.

The ratio $\epsilon (= E_k / E_w)$ is in the range 0.005–0.03. These values indicate that the central star is capable of blowing the interstellar bubble. The figure derived for WR 85 is similar to the ones obtained for most of the H I interstellar bubbles found around O and WR stars. These values support the interpretation that bearing in mind the standard energy conserving model by Weaver et al. (1977), the observed stellar wind energy appears to be too high for the observed bubble dynamics, as pointed out by Cooper et al. (2004), and suggest that the bubbles are most probably in the momentum conserving stage. However, the drain of energy from the bubble through the patchy envelope can not be ruled out.

The ambient density obtained by distributing the total mass within the volume of the bubble (see Section 4.2) is compatible with the value derived for the momentum conserving case ($\sim 3 \text{ cm}^{-3}$).

The SNR G 347.3-0.5 is seen projected onto the same area. The derived distance to the SNR, $d = 6$ kpc, based on molecular line information (Slane et al. 1999), precludes any relation between the SNR and RCW 118 and the H I shell.

5 CONDITIONS FOR STAR FORMATION

The high velocity mass flow produces a drastic change in the physical conditions of the surrounding ISM. Shock fronts linked to stellar winds from massive stars may induce star formation in the high-density regions of the neutral shells, where material has accumulated and conditions for star formation may have been favoured. Then, it is important to analyse the presence of star formation indicators in the neutral shells.

Since protostellar candidates can be identified as infrared sources in the *IRAS* point-source catalogue, we performed a search for *IRAS* point sources projected onto a region of 3° in size centred at the stellar position whose energy distributions are compatible with protostellar objects according to the criteria listed by Junkes, Fürst & Reich (1992). The IR sources found in our search are indicated by triangles in Fig. 7 (left panel). Only the ones within an area of 1° in radius centred at the WR position (triangles with numbers) are listed in Table 3, which shows the source number, its *IRAS* number identification and the fluxes in the four *IRAS* bands.

It is clear from the left panel of the figure that most of the sources are projected onto regions of strong CO emission or close to the galactic plane. The triangles in the right panel of Fig. 7 mark the position of *IRAS* point sources. This panel shows the close correspondence between the IR sources 2, 3, 6, 14, 15, 17 and 18, and the molecular and H I shells linked to RCW 118, suggesting that sequential star formation may be occurring in some sections of the neutral envelope where conditions for stellar formation might have been developed. We note that the distances to these sources are unknown.

6 SUMMARY

We have analysed 21-cm line data belonging to the Southern Galactic Plane Survey searching for an H I bubble related to WR 85 and its ring nebula RCW 118. The main results of our search can be summarized as follows:

(i) The H I data allowed the identification of a cavity in the neutral gas distribution surrounded by a slowly expanding shell. The structure was detected at velocities spanning the interval -28.0 to -16.5 km s^{-1}, and has a systemic velocity of -21 ± 5 km s^{-1}. The cavity can also be identified in the CO emission distribution at similar velocities.

(ii) The ring nebula RCW 118 appears projected onto the inner border of the H I shell.

(iii) The systemic velocity of the H I structure is similar to the velocity of the ionized gas in RCW 118.

(iv) WR 85 is seen in projection onto the central part of the H I cavity and close to its geometrical centre.

(v) The coincidence, within errors, of the kinematical distance to the H I structure and the stellar distance strongly suggests that the WR star is placed within the cavity.

(vi) The morphological coincidence between the inner optical nebula and the H I emission at about -28 km s^{-1} suggests that the 9.3-arcmin nebula is located on the approaching part of the expanding shell. The WR star, which appears closely related to the inner nebula, is also probably located near the approaching part of the shell.

(vii) The CO emission distribution reveals the presence of a molecular shell almost encircling the H I envelope.

(viii) The position of the *IRAS* protostellar candidates projected onto the molecular shell suggests that star formation might be occurring in the region. However, additional studies should be performed to investigate this point.

(ix) The stellar wind of WR 85 is capable of blowing the observed ionized and neutral structure.

The bulk of evidence (i)–(ix) strongly indicates that the H I structure is the neutral gas counterpart of the optical bubble and shows the action of the stellar winds on the surrounding material.

Adopting a distance of 2.8 ± 1.1 kpc, the neutral interstellar bubble has a linear radius of $\sim$21 pc. Taking into account an expansion velocity of 9 ± 2 km s^{-1}, its dynamical age is 1.1×10^6 yr, suggesting that both the present WR star and its massive stellar progenitor have contributed in shaping the bubble. The associated neutral and ionized masses are 3000 M$_\odot$, which indicates that the bubble evolved in a medium with an average ambient density of 3 cm^{-3}.

Table 3. Protostellar candidates within a region of 1° in radius centred on WR 85.

No.	l	b	*IRAS* designation	F(12 μm)	F(25 μm)	F(60 μm)	F(100 μm)
				(Jy)	(Jy)	(Jy)	(Jy)
1	347°4′	-0°4′	17 076-3940	3.75	3.82	131.00	410.00
2	347°4′	-0°22′	17 089-3951	4.38	13.00	98.5	234.00
3	347°4′	-0°13′	17 083-3946	7.94	4.42	39.70	182.00
4	347°12′	-0°6′	17 081-3935	2.75	4.13	94.5	435.00
5	347°15′	-1°22′	17 137-4018	18.89	7.55	63.5	188.00
6	347°15′	-0°33′	17 101-3948	3.25	4.57	18.70	64.59
7	347°17′	-0°1′	17 081-3928	11.00	74.30	221.00	739.00
8	347°17′	0°8′	17 074-3922	3.78	7.38	256.00	1120.00
9	347°25′	0°13′	17 074-3911	4.69	2.42	150.00	397.00
10	347°34′	0°12′	17 079-3905	57.20	396.00	4030.00	8220.00
11	347°38′	0°20′	17 076-3858	2.67	4.03	80.80	280.00
12	347°43′	0°1′	17 091-3905	62.20	24.89	37.5	211.00
13	347°45′	0°9′	17 087-3859	4.00.00	25.10	245.00	628.00
14	347°52′	-0°18′	17 110-3910	3.43	18.29	221.00	941.00
15	347°52′	-0°10′	17 105-3904	1.60	9.10	91.69	226.00
16	347°53′	0°2′	17 096-3856	24.00	164.00	1050.00	1720.00
17	347°55′	-0°45′	17 130-3923	3.49	21.90	145.00	148.00
18	347°58′	-0°25′	17 118-3909	9.72	80.30	1120.00	3000.00
19	348°13′	-0°58′	17 149-3916	209.00	988.00	6760.00	9160.00

REFERENCES

Brand J., Blitz L., 1993, A&A, 275, 67
Cappa C., Goss W. M., Pineault S., 2002, AJ, 123, 3348
Cappa C., Goss W. M., van der Hucht K. A., 2004, AJ, 127, 2885
Cappa C., Arnal M., Cichowolski S., Goss W. M., Pineault S., 2003, in van der Hucht K. A., ed., IAU Symp. 212, A Massive Star Odyssey, from Main Sequence to Supernova. Astron. Soc. Pac., San Francisco, p. 596
Chu Y.-H., Treffers R. R., 1981, ApJ, 250, 615
Chu Y.-H., Treffers R. R., Kwitter K., 1983, ApJS, 53, 937
Condon J. J., Broderick J. J., Seielstad G. A., 1995, ADIL, JC, 6
Conti P. S., Vacca W. D., 1990, AJ, 100, 431
Cooper R. L., Guerrero M. A., Chu Y.-H., Rosie Chen C.-H., Dunne B. C., 2004, ApJ, 605, 751
Dame T. M., Hartmann D., Thaddeus P., 2001, ApJ, 547, 792
Duncan A. R., Stewart R. T., Haynes R. F., Jones K. L., 1995, MNRAS, 277, 36
Gaustad J. E., McCullough P. R., Rosing W., Van Buren D., 2001, PASP, 113, 1326
García-Segura G., Mac Low M.-M., 1995, ApJ, 455, 145
Georgelin Y. M., Georgelin Y. P., 1976, A&A, 49, 57
Haynes R. F., Caswell J. L., Simons L. W. J., 1978, AuJPA, 45, 1
Heckathorn J. N., Bruhweiler F. C., Gull T. R., 1982, ApJ, 252, 230
Junkes N., Fürst E., Reich W., 1992, A&AS, 261, 289
Lamers H. J. G. L. M., Leitherer C., 1993, ApJ, 412, 771
Lazendic J. S., Slane P. O., Gaensler B. M., Reynolds S. P., Plucinsky P. P., Hughes J. P., 2004, ApJ, 602, 271
Marston A. P., Yocum D. R., García-Segura G., Chu Y.-H., 1994a, ApJS, 93, 229
Marston A. P., Yocum D. R., García-Segura G., Chu Y.-H., 1994b, ApJS, 95, 151
Mathis J. S., Cassinelli J. P., van der Hucht K. A., Prusti T., Wesselius P. R., Williams P., 1992, ApJ, 384, 197
McClure-Griffiths N. M., Dickey J. M., Gaensler B. M., Green A. J., Haverkorn M., Strasser S., 2005, ApJ, 158, 178
McCray R., 1983, HiA, 6, 565
Meynet G., Maeder A., 2003, A&A, 404, 975
Mezger P. G., Henderson A. P., 1967, ApJ, 147, 471
Moffat A. F. J., Fitzgerald M. P., 1977, A&A, 54, 263
Pfeffermann E., Aschenbach B., 1996, in Zimmerman H. U., Trümper J., Yorke H., eds, Proc. Röntgenstrahlung from the Universe, MPU, p. 267
Prinja R. K., Barlow M. J., Howarth I. D., 1990, ApJ, 361, 607
Prinja R. K., Fullerton A. W., Crowther P. A., 1996, A&A, 331, 264
Rochowicz K., Nieldzieski A., 1995, AcA, 45, 307
Slane P., Gaensler B. M., Dame T. M., Hughes J. P., Plucinsky P. P., Green A., 1999, ApJ, 525, 357
van der Hucht K., 2001, New astron. Rev., 45, 135
Weaver R., McCray R., Castor J., Shapiro P., Moore R., 1977, ApJ, 218, 377

This paper has been typeset from a TEX/LATEX file prepared by the author.